Macromolecules

ARTICLE

pubs.acs.org/Macromolecules

Long-Range Polymer Chain Dynamics of Pyrene-Labeled Poly(*N*-isopropylacrylamide)s Studied by Fluorescence

Jamie Yip and Jean Duhamel*

Institute of Polymer Research, Department of Chemistry, University of Waterloo, Waterloo, ON N2L 3G1, Canada

Xing Ping Qiu and Françoise M. Winnik*

Faculty of Pharmacy and Department of Chemistry, Université de Montréal, CP 6128 Succursale Centre Ville, Montréal QC H3C 3J7, Canada

Supporting Information

ABSTRACT: The long-range polymer chain dynamics (LRPCD) of poly(*N*-isopropylacrylamide) (PNIPAM) were studied by steady-state and time-resolved fluorescence. Two types of fluorescently labeled PNIPAM constructs were considered. One polymer set, named Py_2−PNIPAM−Y, where 5.6 kDa < Y < 44 kDa is the molecular weight of the polymer, consisted of five monodisperse PNIPAMs that carried 1-pyrenyl-butyl groups at each chain end (functionalization level >75%). The second polymer set consisted of five polydisperse PNIPAMs 75 kDa < M_n < 104 kDa randomly labeled with pyrene (0.1 mol % < pyrene content < 6.0 mol %). Pyrene was selected as its ability to form an excimer from the encounter of two pyrenyl pendants covalently attached onto the polymer yields quantitative information about the LRPCD of a given backbone. The fluorescence data were analyzed according to the Birks scheme for the pyrene end-labeled PNIPAMs and the fluorescence blob model (FBM) for the randomly labeled PNIPAMs. The parameters describing the process of pyrene excimer formation were found to yield equivalent trends regardless of the PNIPAM construct as would be expected since both PNIPAM constructs are essentially pyrene-labeled PNIPAM in nature. Comparison of the parameters describing the LRPCD of PNIPAM and polystyrene obtained with either end- or randomly labeled polymers led to the conclusion that PNIPAM and polystyrene have similar LRPCD in solution as expected from the similarity in bulkiness of their side-chain. This study confirms the claim made first with polystyrene that randomly labeled polymers can be used to obtain quantitative information on the LRPCD of a given polymeric backbone and that they constitute an appealing alternative to end-labeled polymers.

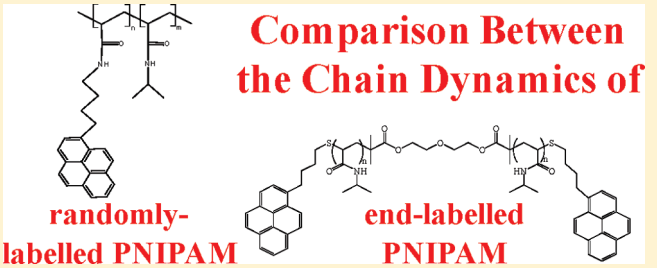

INTRODUCTION

Since the late 1970s,[1−3] fluorescence dynamic quenching experiments have been conducted extensively to study long-range polymer chain dynamics (LRPCD) in solution.[4−7] Early experiments involved the covalent attachment of a luminophore and its quencher to the opposite ends of a monodisperse polymer chain[1,3−5] to take advantage of the theoretical insight brought to the fore by Wilemski and Fixman who predicted that under such conditions, the process of end-to-end cyclization (EEC) can be described by a single rate constant k_{cy}.[8,9] Steady-state and time-resolved fluorescence measurements were then carried out on dilute solutions of the end-labeled polymers to obtain k_q, the rate constant at which the excited luminophore is quenched. Since a fluorescence quenching event indicates that the labeled ends of a same chain have come into contact, k_q is a measure of k_{cy}.

Traditionally, pyrene has been the luminophore of choice to conduct EEC experiments.[1,3−5] The pyrene derivatives that are typically used to label polymers have a relatively high quantum yield (0.32 for pyrene in cyclohexane)[10] and a long lifetime (200−300 ns)[11] in most organic solvents. Quenching occurs when an excited pyrene encounters a ground-state pyrene, a process that results in the formation of a pyrene excimer.[10] Since the pyrene monomer and excimer emit at different wavelengths, the rate constant of excimer formation can be determined with great accuracy by conducting a Birks scheme analysis[5,10] of the pyrene monomer and excimer fluorescence decays when pyrene is attached at both ends of a monodisperse polymer. Additionally, the rate constant of excimer formation provides a measure of k_{cy}.

The use of monodisperse synthetic polymers end-labeled with pyrene[1−24] or other chromophores[25−28] has been instrumental in deepening our understanding of the EEC process, and by extension, long-range polymer chain dynamics (LRPCD). Indeed, the ability to characterize quantitatively polymer chain flexibility through its LRPCD represents an appealing feature in

Received: April 4, 2011
Revised: June 1, 2011
Published: June 15, 2011

the study of protein folding where an EEC event can be viewed as the most basic step taking place in protein folding, namely loop formation.[29−41] However, this method does not come without limitations as a number of recent studies attest. First, EEC can only be probed satisfyingly by pyrene end-labeled polymers that are monodisperse to satisfy the Wilemski and Fixman formalism[8,9] and sufficiently short to ensure that the polymer coil is smaller than the volume V_{blob} probed by an excited pyrene.[42] The former condition is synthetically demanding as monodisperse polymers are usually more difficult to prepare than polydisperse ones, whereas the latter condition which was not considered by Wilemski and Fixman requires that polymer chain length and solvent viscosity be carefully selected as EEC can only be properly studied with short chains in nonviscous solvents. Second, as all EEC studies have found that k_{cy} scales as $\eta^{-1} \times M_n^{-\alpha}$ where η is the solvent viscosity, M_n is the number-average molecular weight, and the scaling exponent α has been found to range from 0.9 to 1.8,[5,12−15,26,38−41] this scaling relationship implies that the number of EEC encounters that can be experimentally probed becomes, in practice, vanishingly small with increasing chain length and solvent viscosity.[11,42] In the case of polystyrene in tetrahydrofuran (η = 0.46 mPa·s), only chains with an M_n smaller than 10 K (i.e., 100 structural units) can be used to study EEC.[3,5]

Work carried out by some of us suggests that all the complications associated with the study of LRPCD via EEC can be circumvented by working with polydisperse polymers randomly labeled with pyrene and analyzing the fluorescence decays of these polymers with the fluorescence blob model (FBM).[7,43] Indeed, the FBM has provided sets of internally consistent parameters that describe quantitatively the LRPCD of pyrene-labeled polystyrene,[11,43−47] poly(*N*,*N*-dimethyl acrylamide),[48−50] or polyisoprene.[51] While these experiments provide valuable information on the LRPCD of the specific polymeric backbones considered, they also create a new pool of data on LRPCD that parallels the vast pool of parameters already obtained from the study of pyrene end-labeled polymers studied with the Birks scheme over the past three decades.[1,3−5,11−24] The two pools were bridged in only one instance where a direct comparison was carried out between the parameters describing the LRPCD of constructs of polydisperse polystyrene randomly labeled with pyrene or monodisperse polystyrene end-labeled with pyrene that were studied with the FBM or the Birks scheme, respectively.[11,45] This comparison suggested that the sets of parameters obtained from both analyses yield equivalent information as long as the parameters are scaled by a fixed coefficient. While this conclusion was interesting as it suggested that the LRPCD of polystyrene can be studied with chains that are labeled with pyrene either at the ends or randomly along the backbone, it was limited to polystyrene.

The numerous advantages associated with the use of randomly labeled polymers to study LRPCD have already been highlighted.[11] However, to ensure that LRPCD can be satisfyingly studied with randomly labeled polymers, the study conducted with polystyrene needs to be generalized by extending it to other polymeric backbones. The present study addresses this issue by considering two series of poly(*N*-isopropylacrylamide) (PNIPAM) constructs, one being constituted of short monodisperse PNIPAM end-capped with pyrene and the other of long polydisperse PNIPAM randomly labeled with pyrene. The steady-state fluorescence spectra and time-resolved fluorescence decays of the PNIPAM constructs were acquired and studied according to the Birks scheme for the end-labeled PNIPAMs[5,10] and the FBM for the randomly labeled PNIPAMs.[7] The results gathered in this work confirm the conclusions that were reached earlier with polystyrene and validate the use of randomly labeled polydisperse polymers as valuable substitutes of end-labeled monodisperse polymers to study LRPCD by fluorescence.

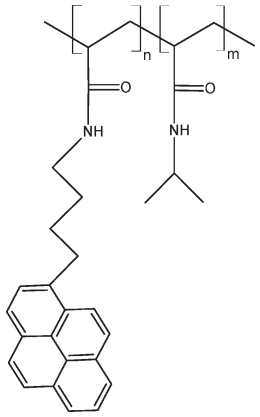

Figure 1. General structure of the randomly labeled Py−PNIPAM−*X*% samples.

EXPERIMENTAL SECTION

Materials. Distilled in glass tetrahydrofuran, high-pressure liquid chromatography (HPLC) grade methanol, and HPLC grade acetonitrile were purchased from Caledon Laboratories. HPLC grade ethanol and hexanol were purchased from Fisher-Scientific. Spectrograde 2-butanone and ethyl acetate were obtained from Aldrich and Honeywell, respectively. Unlabeled PNIPAM used for intrinsic viscosity measurements was purchased from Sigma-Aldrich. Its molecular weight distribution ($\overline{M}_n$ = 95 kDa, PDI = 1.2) was determined by gel permeation chromatography (GPC).[52] All materials were used as received.

Randomly Labeled Poly(*N*-isopropylacrylamide). The general structure of the randomly labeled polymers studied in this project is given in Figure 1. They are referred to as Py−PNIPAM−*X*% where *X* is the pyrene content of polymer in mol %. Their synthesis has been described earlier.[53] The six Py−PNIPAM−*X*% samples were prepared through radical chain copolymerization of *N*-isopropylacrylamide (NIPAM) and *N*-(acryloxy)succinimide (NASI) in *tert*-butyl alcohol, initiated by 2,2-azobis(isobutyronitrile) (AIBN). Copolymerization of NIPAM and NASI yields a random distribution of the two monomers within the polymer and was conducted up to a conversion of 30%. Replacement of the oxysuccinimide group of NASI with [4-(1-pyrenyl)butyl]amine in tetrahydrofuran via nucleophilic acyl substitution at the carbonyl carbon of NASI results in a random distribution of pyrene labels along the polymer backbone. Any excess NASI is subsequently converted to NIPAM via nucleophilic acyl substitution of NASI with *N*-isopropylamine. The pyrene content is then controlled through the amount of [4-(1-pyrenyl)butyl]amine added.

In total, six Py−PNIPAM−*X*% samples were prepared. Their pyrene contents, number-average molecular weights ($\overline{M}_n$), and polydispersity indices (PDI) determined by GPC[52] are listed in Table 1.

End-Labeled Poly(*N*-isopropylacrylamide). The structures of the end-labeled PNIPAM samples (Py_2−PNIPAM−Y and

Py_1−PNIPAM) are shown in Figure 2. Their synthesis has been described earlier and is briefly presented hereafter.[54,55] The Py_2−PNIPAM−Y samples were synthesized through a reversible addition−fragmentation chain transfer (RAFT) polymerization of *N*-isopropylacrylamide initiated with AIBN. The reversible chain transfer agents were either diethylene glycol di(2-(1-isobutyl)sulfanylthiocarbonylsulfanyl-2-methylpropionate) (DEGDIM) for the synthesis of Py_2−PNIPAM−Y or ethyl 2-(1-isobutyl)sulfanylthiocarbonyl-2-methyl propionate for the synthesis of Py_1−PNIPAM. The RAFT polymerization with DEGDIM results in the formation of α,ω-di-isobutyldithiocarbonylthio PNIPAM. Aminolysis of the isobutyldithiocarbonylthio end groups using *n*-butylamine leads to α,ω-dimercapto−PNIPAM. Reaction of the mercapto end groups with 4-(1-pyrenyl)butyl iodide yields a Py_2−PNIPAM (Figure 2). Polymerization of NIPAM in the presence of ethyl 2-(1-isobutyl)sulfanylthiocarbonyl-2-methyl propionate leads to a polymer bearing a methyl propionate group at one end and an isobutylthiocarbonylthio group at the other end. Aminolysis of the thiocarbonylthio group with *n*-butyl amine followed by reaction with pyrenylbutyl iodide yields Py_1−PNIPAM (Figure 2).

In total, five pyrene di-end-labeled samples and one monolabeled sample (Py_1−PNIPAM−25K) were synthesized. The monolabeled sample was used as a model compound to determine the natural lifetime of pyrene attached to the PNIPAM chain. Their pyrene functionalities, $\overline{M}_n$, and PDI values determined by GPC[52] are listed in Table 2. All end-labeled samples were monodisperse, with PDI values less than or equal to 1.10.

Intrinsic Viscosity Measurements. A sample of unlabeled PNIPAM ($\overline{M}_n$ = 95 kDa, PDI = 1.2) was used to gauge the quality of different organic solvents toward PNIPAM by conducting intrinsic viscosity measurements. Five concentrations ranging from 2 to 10 g/L were used in order to measure the intrinsic viscosity of PNIPAM in each solvent and solvent mixture. Measurements were done with an Übbelohde viscometer placed in an ethylene glycol/water bath maintained at a constant temperature of 25 ± 0.5 °C. Intrinsic viscosities of PNIPAM in each solvent are given in Table 3.

Viscosities of Binary Mixtures of Methanol and Hexanol. A calibration curve was constructed using an Übbelohde viscometer to estimate the viscosities of binary mixtures of methanol and hexanol as a function of the methanol content. The relation-

Table 1. Pyrene Contents, Molecular Weights, and Polydispersity Indices of the Py−PNIPAM−*X*% Samples

sample	Py content (mol %)	Py content (λ_{Py} in μmol·g^{-1})	$\overline{M}_n$ (kDa)	PDI
Py−PNIPAM−0.1%	0.12	10	104.0	1.75
Py−PNIPAM−2%	2.7	230	92.4	1.57
Py−PNIPAM−3%	3.6	300	71.0	1.63
Py−PNIPAM−4%	4.2	340	81.4	1.37
Py−PNIPAM−5%	5.1	410	70.5	1.70
Py−PNIPAM−6%	6.3	500	73.3	1.55

Table 2. Pyrene Functionalities, Pyrene Contents, Molecular Weights, and Polydispersity Indices of the End-Labeled Py_2−PNIPAM−Y Samples

sample	pyrene functionality (%)	Py content (λ_{Py} in μmol.g^{-1})	$\overline{M}_n$ (kDa)	PDI
Py_2−PNIPAM−6K	85.4	290	5.9	1.05
Py_2−PNIPAM−8K	82.6	244	7.6	1.08
Py_2−PNIPAM−14K	87.4	140	13.7	1.10
Py_2−PNIPAM−25K	75.5	65	25.4	1.07
Py_2−PNIPAM−45K	74.8	31	44.5	1.10
Py_1−PNIPAM−25K	--		23.5	1.09

Table 3. Viscosities and Densities of, as Well as Intrinsic Viscosities of the Unlabeled PNIPAM Sample in the Solvents Used in This Study

solvent	η (mPa·s)	ρ (g/mL)	$[\eta]$ (dL·g^{-1})
acetonitrile	0.37	0.78	2.09 ± 0.02
2-butanone	0.41	0.81	2.99 ± 0.06
ethyl acetate[a]	0.42	0.90	
tetrahydrofuran	0.46	0.88	3.55 ± 0.03
methanol	0.54	0.79	4.31 ± 0.06
80% methanol/hexanol	0.71	0.79	4.66 ± 0.04
60% methanol/hexanol	0.97	0.80	5.04 ± 0.06
ethanol	1.1	0.79	4.85 ± 0.05
30% methanol/hexanol	1.7	0.81	5.4 ± 0.1
15% methanol/hexanol	2.6	0.81	5.3 ± 0.1
6% methanol/hexanol	3.6	0.81	5.6 ± 0.1
hexanol	4.6	0.82	6.0 ± 0.2

[a] PNIPAM is not soluble enough in ethyl acetate to conduct intrinsic viscosity measurements.

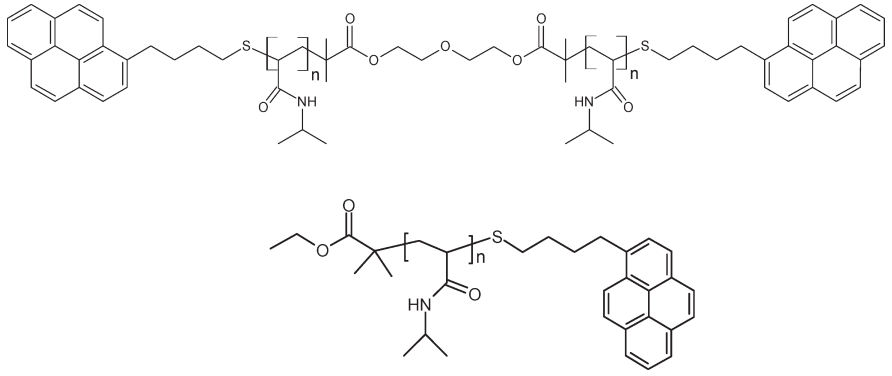

Figure 2. General structure of the pyrene end-labeled polymers Py_2−PNIPAM−Y and Py_1−PNIPAM.

dx.doi.org/10.1021/ma2007865 |*Macromolecules* 2011, 44, 5363–5372

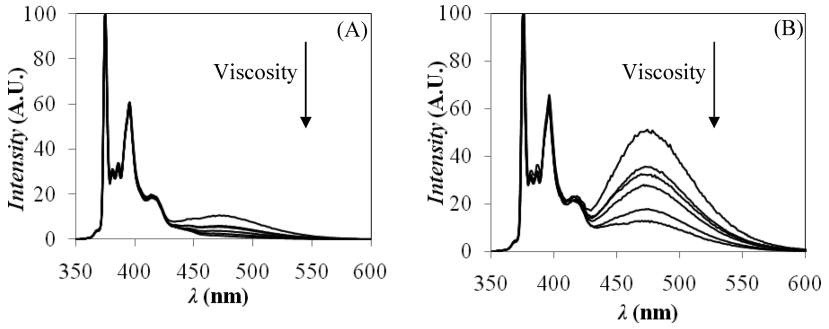

Figure 3. Steady-state fluorescence spectra for (A) Py_2—PNIPAM—6K and (B) Py—PNIPAM—3%. λ_{ex} = 344 nm, [Py] = 2.5 μM. Top to bottom: methanol (η = 0.55 mPa·s), 80% methanol/hexanol (η = 0.71 mPa·s), ethanol (η = 1.1 mPa·s), 60% methanol/hexanol (η = 0.97 mPa·s), 30% methanol/hexanol (η = 1.7 mPa·s), and hexanol (η = 4.6 mPa·s).

ship between the viscosity (η) of the solvent mixture and the methanol content v in vol % is given in eq 1.

$$\eta = 13.251v^4 - 35.045v^3 + 34.845v^2 - 16.98v + 4.4975 \quad (1)$$

UV—Visible Absorbance Measurements. UV—visible absorbances were measured on a Cary 100 UV—vis spectrophotometer with an absorption cell having a 1 cm path length. Absorbances were measured in the 200—600 nm wavelength range. All PNIPAM solutions used for fluorescence measurements had an absorbance at 344 nm of less than 0.1, corresponding to a pyrene concentration smaller than 2.5 μM. This pyrene concentration ensures that excimer formation occurs intra- and not intermolecularly. The pyrene content of the Py—PNIPAM—X% samples (λ_{Py} in μmol/g in Table 1) was measured by UV—vis spectrophotometry using the molar extinction coefficient of 1-pyrenebutanol in ethanol (43 000 $M^{-1}\cdot cm^{-1}$ at 344 nm).[56] λ_{Py} was then used to determine the mole fraction x of pyrene labeled units in the polymer sample according to eq 2.

$$x = \frac{M_1}{M_1 - M_2 + \frac{1}{\lambda_{Py}}} \quad (2)$$

where M_1 and M_2 represent the molar masses of the labeled (326 $g\cdot mol^{-1}$) and unlabeled (113 $g\cdot mol^{-1}$) NIPAM monomers, respectively.

Steady-State Fluorescence Measurements. Steady-state fluorescence spectra of the pyrene-labeled PNIPAM samples were acquired on a Photon Technology International (PTI) LS-100 steady-state fluorometer equipped with an Ushio UXL-75Xe Xenon arc lamp and a PTI 814 photomultiplier detection system. The solutions were excited at 344 nm and their emission was monitored from 350 to 600 nm. All solutions were degassed under a steady stream of nitrogen for 30 min and had a pyrene concentration smaller than 2.5 μM, sufficiently dilute to prevent intermolecular excimer formation. The monomer fluorescence intensity (I_M) was obtained by taking the integral under the fluorescence spectrum from 372 to 378 nm. The fluorescence intensity of the excimer (I_E) was determined by first acquiring the steady-state fluorescence spectrum of the monolabeled Py_1—PNIPAM—25K sample. Next, the fluorescence spectrum of Py_1—PNIPAM—25K was subtracted from the spectrum of the randomly or end-labeled PNIPAM sample. Finally, I_E was calculated by taking the integral of the subtracted spectrum from 500 to 530 nm.

Time-Resolved Fluorescence Measurements. The fluorescence decays of the pyrene monomer and excimer of the pyrene-labeled PNIPAM solutions were acquired on an IBH time-resolved fluorometer equipped with a nano-LED light source. The solutions were prepared with a pyrene concentration of approximately 2.5 μM, small enough to ensure that no intermolecular excimer formation was being observed. The solutions were excited at a wavelength of 344 nm and emission was monitored at 375 and 510 nm for the pyrene monomer and excimer using a cutoff filter at 370 and 495 nm, respectively. A Ludox solution was used at the excitation wavelength to determine the instrument response function which was convoluted with the desired theoretical function for the decay analysis. Fluorescence decays of the Py_2—PNIPAM—Y and Py—PNIPAM—X% samples were analyzed using the Birks Scheme[5,10] with eqs S.1 and S.2 in the Supporting Information and the FBM[7,43] with eqs S.5 and S.6 in the Supporting Information, respectively. A complete description of both models is given in Supporting Information, together with the definition of all parameters used in these analyses.

RESULTS AND DISCUSSION

Dilute solutions of the end-labeled Py_2—PNIPAM—6K and randomly labeled Py—PNIPAM—3% polymers were prepared in all organic solvents considered. Their fluorescence spectra were acquired and normalized to the peak at 375 nm. The normalized spectra are shown in Figure 3. Typical monomer emission peaks are observed in the 370 to 425 nm wavelength region, while the excimer emission is seen as a broad, structureless emission centered around 470 nm. Direct comparison of Figures 3A and 3B demonstrates that excimer emission of the Py—PNIPAM—3% sample is significantly stronger than that of the Py_2—PNIPAM—6K sample, even though the two polymers have similar pyrene contents (cf. Tables 1 and 2). Most importantly, the excimer signal of Py_2—PNIPAM—6K, a polymer constituted of about 55 structural units, is strongly reduced and can hardly be detected in organic solvents having a viscosity larger than 1 mPa·s. This effect is due to the architecture of the pyrene end-labeled polymer constructs which holds the pyrene labels far apart from each other. By contrast, the randomly labeled polymer contains many pairs of pyrene labels, some of which being separated by shorter chain segments and capable of generating excimer more effectively even in the most viscous solvents. In turn, this effect confirms the inherent superiority of randomly

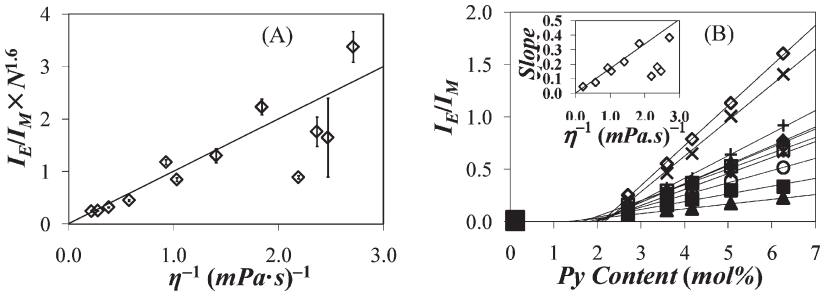

Figure 4. (A) Plot of $I_E/I_M \times N^{1.6}$ as a function of η^{-1} averaged for the Py_2−PNIPAM−6K, Py_2−PNIPAM−8K, and Py_2−PNIPAM−14K samples. (B) Plot of I_E/I_M as a function of pyrene content for the Py−PNIPAM−X% samples in acetonitrile (◊), 2-butanone (□), ethyl acetate (Δ), tetrahydrofuran (○), methanol (×), 80% methanol/hexanol (+), 60% methanol/hexanol (∗), ethanol (◆), 30% methanol/hexanol (■), and hexanol (▲). Inset: Slopes of the lines shown in Figure 4B plotted as a function of η^{-1}.

labeled polymeric constructs when excimer formation is monitored to study LRPCD as it was suggested earlier for a series of polystyrenes randomly end-labeled with pyrene.[11]

The fluorescence spectra of all pyrene-labeled polymers were acquired and the ratios of the fluorescence intensity of the pyrene excimer over that of the pyrene monomer, namely the I_E/I_M ratios, were determined. They are plotted as a function of the inverse of viscosity (η^{-1}) in Figure 4. For quantitative analysis of the pyrene end-labeled PNIPAMs, however, only the short PNIPAM constructs, namely Py_2−PNIPAM−6K, Py_2−PNIPAM−8K, and Py_2−PNIPAM−14K, were considered, as the longer constructs yielded hardly any excimer. The I_E/I_M trends of the shorter PNIPAM constructs shown in Figure 4A illustrate the difference of the protic versus aprotic nature of the solvent. Whereas I_E/I_M appears to be inversely proportional to the solvent viscosity when alcohols are used (all data points with $\eta^{-1} < 1.84$ mPa^{-1}·s^{-1}), the I_E/I_M ratios are much more scattered in the aprotic solvents used to attain viscosities smaller than that of methanol ($\eta = 0.54$ mPa·s). Whereas the I_E/I_M ratio in acetonitrile ($\eta^{-1} = 2.70$ mPa^{-1}·s^{-1}) is close to the straight line defined by the protic solvents, the I_E/I_M ratios obtained in THF ($\eta^{-1} = 2.17$ mPa^{-1}·s^{-1}), 2-butanone ($\eta^{-1} = 2.44$ mPa^{-1}·s^{-1}), and ethyl acetate ($\eta^{-1} = 2.38$ mPa^{-1}·s^{-1}) are clearly off the line. Incidentally, the quality of these solvents toward PNIPAM is also much poorer than that of the alcohols as inferred from the intrinsic viscosity measurements (Table 3). Consequently, only the results obtained with the PNIPAM samples in alcohol solutions will be considered from now on. The product $\eta \times I_E/I_M$ of the end-labeled polymers in the alcohols was found to scale as $M_n^{-1.6\pm0.3}$ in Figure 4A, in perfect agreement with the $I_E/I_M \sim M_n^{-\alpha}$ relationships reported in the literature where α takes values between 0.9 and 1.9.[5,12−15,26,38−41]

The I_E/I_M ratio of the randomly labeled polymers is shown in Figure 4B as a function of pyrene content. After an onset pyrene content of about 2 mol %, the I_E/I_M ratio increased linearly with increasing pyrene content, with a steeper increase being observed for the less viscous solvents. The trends shown in Figure 4B indicate that a minimum level of pyrene labeling is necessary to bring the pyrene labels close enough from each other in order to induce excimer formation. While such a result would be expected, the PNIPAM samples randomly labeled with pyrene represent the first example of a pyrene-labeled polymeric construct for which so pronounced an onset pyrene content is found before excimer formation is observed.

The slope of the straight lines representing the I_E/I_M ratio vs pyrene content shown in Figure 4B is a measure of the efficiency of the randomly labeled PNIPAM at forming excimer, and it is expected to depend on solvent viscosity. The slopes of the lines were determined and they are plotted as a function of η^{-1} in the inset of Figure 4B. This plot is identical to that shown in Figure 4A for the pyrene end-labeled PNIPAMs, with the data obtained in the protic solvents lining up nicely on a straight line while the results obtained in the aprotic solvents are scattered. The excellent agreement observed between Figure 4A obtained with the end-labeled PNIPAMs and the inset of Figure 4B obtained for the randomly labeled PNIPAMs suggests that the process of excimer formation studied for both constructs yield the same information on LRPCD.

The fluorescence decays of the pyrene monomer and excimer of the end− and randomly labeled PNIPAMs were fitted with the set of eqs S.1 and S.2 in the Supporting Information for the Birks' scheme analysis and the set of eqs S.5 and S.6 in the Supporting Information for the FBM analysis, respectively. The parameters retrieved from these analyses are listed in Tables S.1−S.15 in the Supporting Information. The parameters obtained with the Birks scheme analysis of the fluorescence decays acquired with the Py_2−PNIPAM−Y constructs are discussed first.

According to the Birks scheme, the process of excimer formation between the two pyrene-labeled ends of the Py_2−PNIPAM−Y samples is described by the EEC rate constant, k_{cy}, the rate constant of excimer dissociation, k_{-cy}, the excimer lifetime, τ_E, and the molar fraction of pyrene pendants that are attached on singly labeled chains and cannot form excimer, f_{Mfree}. The parameters k_{cy}, k_{-cy}, τ_E, and f_{Mfree} were found to depend on solvent viscosity (η) and polymer chain length (N). Their scaling behavior as a function of N and η was established following a procedure that has been described earlier and it is shown in Figure 5.[46] For short chains and low solvent viscosities, k_{cy} decreases with increasing viscosity and molecular weight, as expected.[5,12−15,26,38−41] But for long polymer chains and large solvent viscosities, k_{cy} plateaus. In particular, k_{cy} hardly changes with solvent viscosity for the Py_2−PNIPAM−14K sample (triangles). The excimer dissociation rate constant k_{-cy} increases linearly with increasing viscosity and chain length, but remains smaller than 5.0×10^6 s^{-1} for $\eta \times N$ products smaller than ∼60 mPa·s, i.e. for relatively short chains and small solvent viscosities. On the basis of the exponents found in Figure 5C, the excimer lifetime τ_E depends little on viscosity and polymer chain length, and for $\eta \times N$ products smaller than ∼60 mPa·s, τ_E is found to equal 62 ± 4 ns which is a reasonable value for a pyrene excimer in organic solvents.[10] For longer chains and larger solvent viscosities, however, τ_E increases to unexpectedly large values. The fraction of monolabeled chains, f_{Mfree} remains

dx.doi.org/10.1021/ma2007865 |Macromolecules 2011, 44, 5363–5372

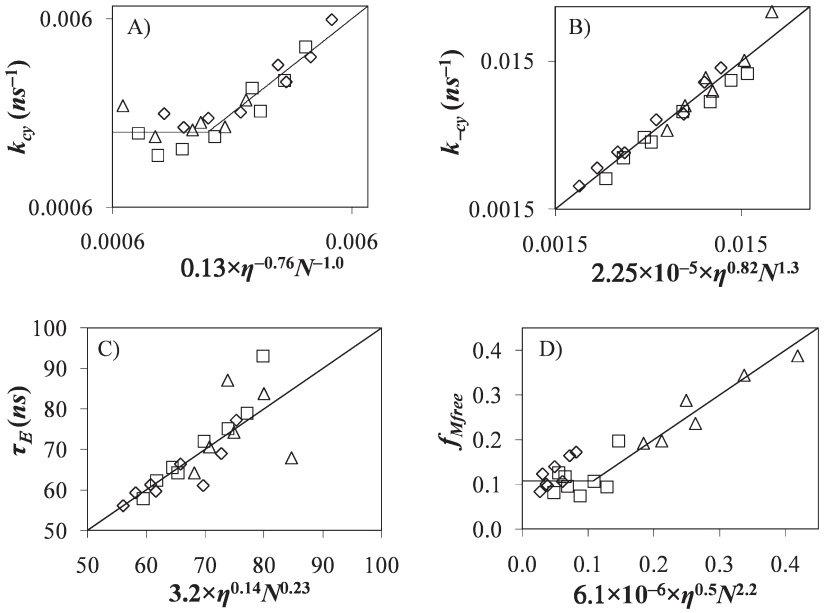

Figure 5. Scaling relationships for (A) k_{cy}, (B) k_{-cy}, (C) τ_E, and (D) f_{Mfree} for Py_2−PNIPAM−6K (◇), Py_2−PNIPAM−8K (□), and Py_2−PNIPAM−14K (Δ). The errors on the exponents are listed in Table S.16 in the Supporting Information.

constant and equal to 0.11 ± 0.03 for Py_2−PNIPAM−6K and Py_2−PNIPAM−8K, but for Py_2−PNIPAM−14K, f_{Mfree} increases with increasing viscosity.

The trends shown in Figure 5, parts A−D, highlight some serious deficiencies of the Birks scheme analysis. First, k_{cy} is expected to decrease continuously with increasing viscosity and polymer chain length. Second, k_{-cy} and τ_E do not depend on viscosity and polymer chain length for long chains as only a few structural units beside the pyrene labels are expected to affect their values. Consequently, k_{-cy} and τ_E should remain constant in Figure 5, parts B and C, at the very least for the largest PNIPAM constructs, as they describe the photophysical properties of the pyrene excimer. Third, the fraction of monolabeled chains f_{Mfree} is an intrinsic property of the polymer sample which cannot double with increasing solvent viscosity as it does with Py_2−PNIPAM−14K (Figure 5D). Although the k_{cy}, k_{-cy}, τ_E, and f_{Mfree} parameters retrieved for short chains and small solvent viscosities appear to behave somewhat reasonably, Birks' scheme clearly breaks down for longer chains and larger solvent viscosities. These observations agree closely with those reported recently for a series of pyrene end-labeled poly(ethylene oxide) (Py_2−PEO)[42] and suggest that the effect described in Figure 5, parts A−D, is general.

In the case of Py_2−PEO, the breakdown of Birks scheme for long chains and/or viscous solvents was traced back to the partitioning of the pyrenyl ends in the polymer coil.[42] If the ground-state pyrene at one polymer end is located inside the volume V_{blob} probed by the excited pyrene at the other end,[7] excimer formation occurs with a rate constant k_{blob}. But if the ground-state pyrene is located outside a blob, it might be incapable of forming an excimer resulting in a large f_{Mfree} value which increases with increasing polymer chain length and/or solvent viscosity, as observed for Py_2−PNIPAM−14K in Figure 5D. The similarity in the trends shown in Figure 5 for the Py_2−PNIPAM samples and those found for the Py_2-PEO samples suggests that a same phenomenon might be at play. A detailed overview about the application of the FBM to the study of pyrene end-labeled polymers can be found in a recent publication.[42]

The fluorescence decays of the PNIPAM samples randomly labeled with pyrene were fit using the Fluorescence Blob Model according to eqs S.5 and S.6 in the Supporting Information. In the analysis, the monomer lifetime τ_M was fixed to the value determined by acquiring the fluorescence decays of the Py−PNIPAM−0.1% sample, fitting the decay using a sum of two exponentials, and taking the longest decaytime obtained with the largest pre-exponential factor as the monomer lifetime. Within the framework of the FBM, excimer formation occurs sequentially where slow diffusive encounters of the polymer units bearing a pyrenyl pendant are followed by their rapid rearrangement to form an excimer. Diffusive encounters are described by the FBM parameters which are k_{blob}, the rate constant of excimer formation inside a blob containing one ground-state and one excited pyrene, $\langle n \rangle$, the average number of pyrenes per blob, and $k_e \times$ [blob] which describes the rate at which ground-state pyrenes exchange between blobs. The parameter $\langle n \rangle$ is used to determine the blob size, N_{blob}, whose exact definition is given in eq S.10 in the Supporting Information. The rapid rearrangement of the pyrenyl pendants into an excimer is described by the rate constant k_2. It was determined by letting k_2 float in a first analysis, averaging the values obtained for each pyrene content, and then fixing k_2 to its average value in a subsequent analysis. The parameters retrieved from this analysis are listed in Tables S.6−S.15 in the Supporting Information. Figures 6A - D represent plots of the parameters $k_e \times$ [blob], k_{blob}, N_{blob}, and $k_{blob} \times N_{blob}$ as a function of the corrected pyrene content, $\lambda_{Py}/(1 - f_{Mfree})$. The factor $(1 - f_{Mfree})^{-1}$ accounts for the larger local concentration experienced by those excited pyrenes located in pyrene-rich domains of the polymer coil when pyrene-poor domains exist where a molar fraction f_{Mfree} of the pyrene monomers are isolated along the polymer backbone and cannot form excimer.[7]

Except for $k_e \times$ [blob] which is usually retrieved with more scatter, k_{blob}, N_{blob}, and $k_{blob} \times N_{blob}$ appear to remain constant

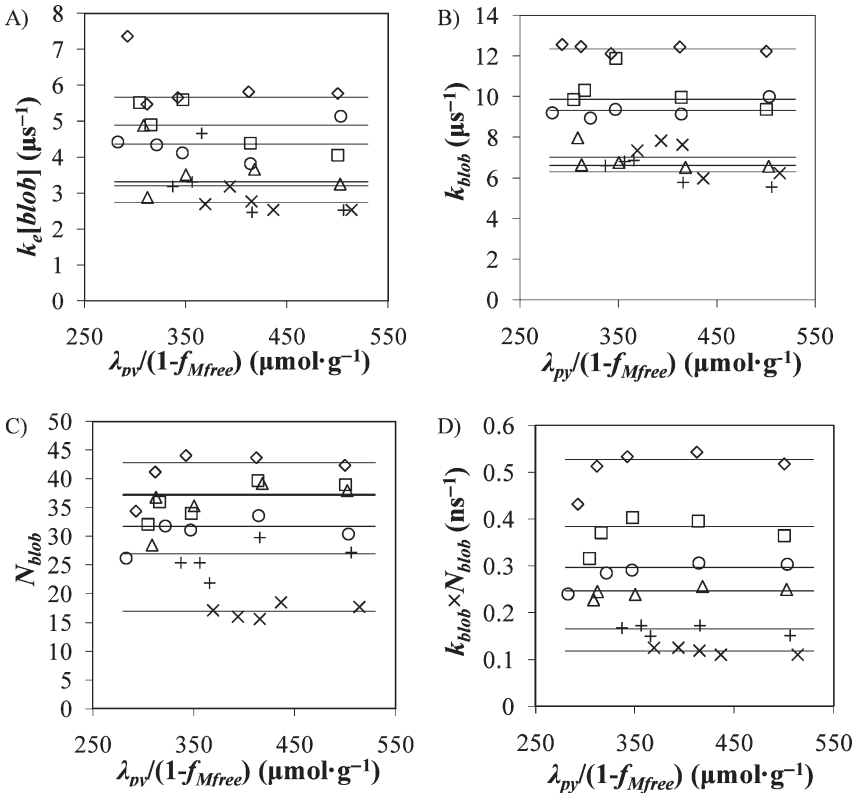

Figure 6. Plots of (A) $k_e \times$ [blob], (B) k_{blob}, (C) N_{blob}, and (D) $k_{blob} \times N_{blob}$ as a function of the corrected pyrene content in MeOH (◇), 80% MeOH (□), 60% MeOH (Δ), ethanol (○), 30% MeOH (+), and hexanol (×).

with pyrene content, with a small variation (usually a dip) observed in some instances for Py−PNIPAM−2%. We suspect that this variation with respect to the other PNIPAM samples is due to Py−PNIPAM−2% having a pyrene content that is too close to the break point found in the I_E/I_M trends shown in Figure 4B. Indeed, f_{free}, the molar fraction of isolated pyrenes that cannot form excimer, is consistently larger for Py−PNIPAM−2% in Tables S.6-S.15 in the Supporting Information, reflecting the larger average spacing between pyrene pendants in this sample. Ignoring the values retrieved for the Py−PNIPAM−2% sample, the remaining values were averaged to yield $\langle k_e \times [\text{blob}]\rangle$, $\langle k_{blob}\rangle$, $\langle N_{blob}\rangle$, and $\langle k_{blob} \times N_{blob}\rangle$. They are shown as a function of η^{-1} in Figure 7 together with the same parameters obtained earlier for polystyrene randomly labeled with 1-pyrenebutanol via the copolymerization of styrene and 1-pyrenebutyl acrylate.[47] Since the type and choice of incorporation of pyrene derivatives have been shown to affect profoundly the process of excimer formation for pyrene-labeled polymers,[11,44−47] the similarity in the pyrene derivatives used to label PNIPAM in the present study and PS ensures that the trends can be compared quantitatively. The data shown for PS in Figure 7 were obtained in a earlier publication in toluene, *N*,*N*-dimethylformamide, dioxane, dimethylacetamide, and benzyl alcohol whose respective viscosity equals 0.56, 0.79, 1.18, 1.93, and 5.47 mPa·s.[47]

The rate constant $\langle k_e[\text{blob}]\rangle$ describing the exchange of pyrenes between blobs is smaller than $\langle k_{blob}\rangle$ indicating that a ground-state pyrene present in a blob is likelier to quench the excited pyrene rather than escape the blob. Both $\langle k_e[\text{blob}]\rangle$ and $\langle k_{blob}\rangle$ do not change much with viscosity, as expected within the framework of the FBM.[44−50] In the case of k_e[blob], the concentration of blobs inside the polymer coil increases as the viscosity increases since the blobs become smaller but the volume of the polymer coil remains constant. However k_e which is the rate constant describing the diffusive exchange of ground-state pyrenes between blobs decreases as it is inversely proportional to the solvent viscosity, thus canceling the increase in [blob] and resulting in a k_e[blob], which depends little on solvent viscosity as found in Figure 7A. By its definition, k_{blob} is a pseudounimolecular rate constant which is the product of the rate constant describing the bimolecular encounter between an excited pyrene and a ground-state pyrene multiplied by the concentration equivalent to one ground-state pyrene located inside a blob of volume V_{blob}. The expression of k_{blob} is given in eq 3.

$$k_{blob} = k_{diff} \times \frac{1}{V_{blob}} \qquad (3)$$

As the viscosity increases, V_{blob} decreases and k_{diff} which is inversely proportional to the solvent viscosity decreases. Both effects cancel each other resulting in the trend shown in Figure 7B for $\langle k_{blob}\rangle$. As the solvent viscosity decreases, the excited pyrene probes a larger V_{blob} and a larger N_{blob} value is obtained as observed in Figure 7C. Finally, the product $\langle k_{blob} \times N_{blob}\rangle$, which has been shown to describe the LRPCD of a given polymer is found to be inversely proportional to solvent viscosity, as expected from a diffusion-controlled process.[11,15] Together, the parameters $\langle k_e \times [\text{blob}]\rangle$, $\langle k_{blob}\rangle$, $\langle N_{blob}\rangle$, and $\langle k_{blob} \times N_{blob}\rangle$ provide an accurate description of the LRPCD of PNIPAM. In particular, they can be used to compare quantitatively the LRPCD of PNIPAM with polystyrene. Over the range of solvent viscosities studied for PNIPAM, namely 0.54 mPa·s for methanol and 4.6 mPa·s for hexanol, $\langle k_e[\text{blob}]\rangle$, $\langle N_{blob}\rangle$, and $\langle k_{blob} \times N_{blob}\rangle$ are consistently smaller for PNIPAM than for polystyrene.

dx.doi.org/10.1021/ma2007865 |*Macromolecules* 2011, 44, 5363–5372

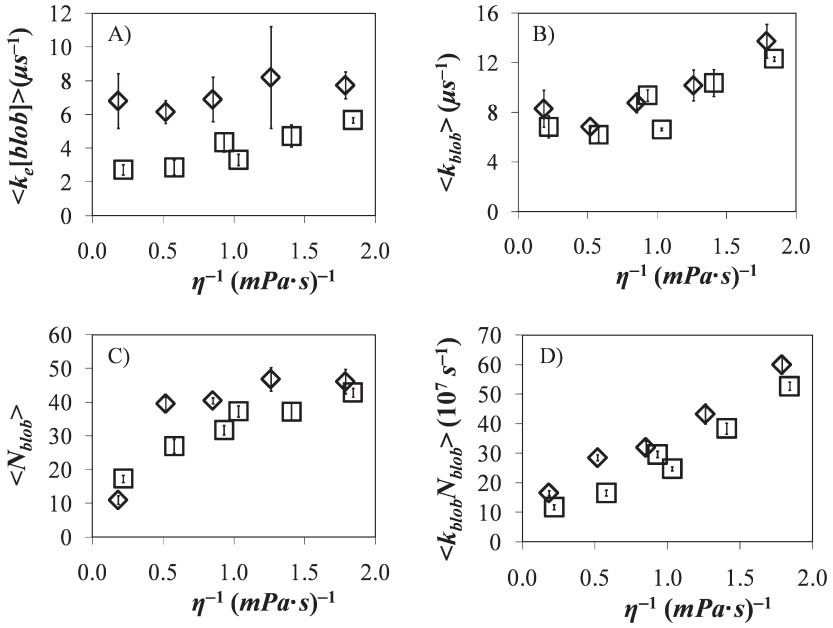

Figure 7. Average values of (A) $k_e \times$ [blob], (B) k_{blob}, (C) N_{blob}, and (D) $k_{blob} \times N_{blob}$ obtained in Figure 6 and plotted as a function of η^{-1}. Key: (□) PNIPAM; (◇) polystyrene.

Since the product $\langle k_{blob} \times N_{blob}\rangle$ reflects the LRPCD,[11,44−47] our results based on the randomly labeled PNIPAM indicate that polystyrene is about 10% ($\langle k_{blob} \times N_{blob}\rangle^{PS}/\langle k_{blob} \times N_{blob}\rangle^{PNIPAM}$ = 1.10) more flexible than PNIPAM in protic solvents.

In an earlier study carried out with polystyrene randomly labeled with 1-pyrenebutanol,[47] the product $\langle k_{blob} \times N_{blob}\rangle$ was found to be on average 3.2 times larger than the product $\langle k_{cy} \times N\rangle$ where N is the number-average degree of polymerization of three short polystyrene constructs end-labeled with 1-pyrenebutylamine.[11] In the case of the randomly labeled PNIPAM, the product $\langle k_{blob} \times N_{blob}\rangle$ is found to be 1.8 times larger than $\langle k_{cy} \times N\rangle$ for the two shortest end-labeled PNIPAMs, namely Py_2−PNIPAM−6K and Py_2−PNIPAM−8K since k_{cy} for Py_2−PNIPAM−14K has been shown to behave somewhat unexpectedly in Figure 5A. A plot comparing $\langle k_{blob} \times N_{blob}\rangle$ and 1.8 × $\langle k_{cy} \times N\rangle$ for PNIPAM is shown as a function of η^{-1} in Figure 8.

The agreement between the two sets of data is remarkable, as was obtained for polystyrene.[11] In particular, both $\langle k_{blob} \times N_{blob}\rangle$ and $\langle k_{cy} \times N\rangle$ take a slightly larger value than expected in ethanol (η = 1.1 mPa·s), suggesting that both constructs respond to the solvent in the same manner. However, whereas the $\langle k_{blob} \times N_{blob}\rangle$ values obtained for the randomly labeled polymers indicated that polystyrene is about 10% stiffer than PNIPAM in protic solvents ($\langle k_{blob} \times N_{blob}\rangle^{PS}/\langle k_{blob} \times N_{blob}\rangle^{PNIPAM}$ = 1.10), the $\langle k_{cy} \times N\rangle$ trends yield an opposite result with polystyrene being about 33% ($\langle k_{cy} \times N\rangle^{PS}/\langle k_{cy} \times N\rangle^{PNIPAM}$ = 0.67) more flexible than PNIPAM.

Although the exact origin of this discrepancy is difficult to assess at the present time, it illustrates the sensitivity of fluorescence in general and pyrene excimer formation in particular to minute differences in the overall chemical structure of the pyrene-labeled polymer constructs, an already well-described observation.[11,44−47] On the one hand, the amide linkers used to connect the 1-pyrenebutyl derivatives to the ends of polystyrene in ref 11 might slow down the process of excimer formation. On the other hand, the diethylene glycol segment

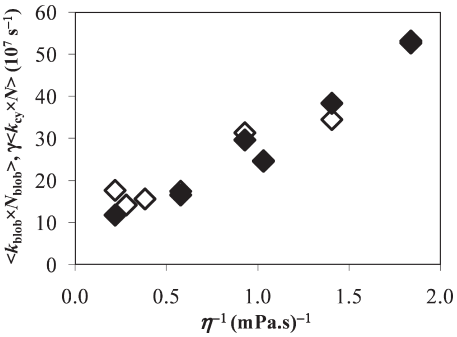

Figure 8. Plot of $\langle k_{blob} \times N_{blob}\rangle$ (◇) and $\gamma \cdot \langle k_{cy} \times N\rangle$ (◆) for PNIPAM as functions of η^{-1} where γ equals 1.8.

located at the core of the Py_2−PNIPAM−Y samples together with the flexible thio ether linkage used to connect the 1-pyrenebutyl derivative to the ends of PNIPAM might enhance the overall flexibility of the chain and favor excimer formation. In any case, whether polystyrene might be 10% stiffer or 33% more flexible than PNIPAM, these results suggest that these polymeric backbones have similar flexibilities as would be expected from their similar characteristic ratios C_∞ reported to be 10.2 for polystyrene in cyclohexane at 34.5 °C[57] and 10.6 for PNIPAM in THF at 25 °C.[58] In comparison, recent results obtained with pyrene end-labeled monodisperse poly(ethylene oxide) (PEO) yield $\langle k_{cy} \times N\rangle^{PEO}$ values that are 2.4 and 3.8 times larger than $\langle k_{cy} \times N\rangle^{PNIPAM}$ and $\langle k_{cy} \times N\rangle^{PS}$, respectively (see Figure S1 in Supporting Information).[42] Furthermore, considering that each structural unit of PEO contributes three atoms to the backbone versus two for PNIPAM and PS, the product $n \times \langle k_{cy} \times N\rangle^{PEO}$, where n is the number of backbone atoms per structural unit, is actually 3.6 and 5.7 times larger than $n \times \langle k_{cy} \times N\rangle^{PNIPAM}$ and $n \times \langle k_{cy} \times N\rangle^{PS}$, respectively. PEO having a characteristic ratio of

3.8[59] is much more flexible than PS and PNIPAM, and as a result yields much larger $n \times \langle k_{cy} \times N \rangle^{PEO}$ values.

The LRPCD described in this study were monitored for pyrene-labeled PNIPAMs in solvent mixtures of methanol and hexanol. One problem associated with the use of solvent mixtures revolves about the preferential adsorption of one of the two solvents onto the polymer of interest. When such specific solvent effects occur, the bulk viscosity of the solvent mixture can no longer represent the viscosity experienced locally by the chain. To investigate the extent to which this might be happening in our experiments, the PNIPAM samples were studied in ethanol, a homogeneous solvent of 1.1 mPa·s viscosity similar to that of a methanol:hexanol mixture containing 54 vol % of methanol. Although the results obtained in ethanol appear to be slightly off the trend obtained with the solvent mixtures (see Figures 4 and 8) suggesting a slightly enhanced excimer formation in ethanol, the difference is small and could also be related to a worsening of the solvent quality toward PNIPAM in ethanol as well as some preferential adsorption of one of the solvents of the solvent mixture. According to the data listed in Table 3, the intrinsic viscosity of PNIPAM in ethanol is smaller than that in the methanol:hexanol mixture. Thus, the local concentration of pyrene in the pyrene-labeled PNIPAM constructs is higher in ethanol than in the solvent mixture resulting in a larger rate of excimer formation as reflected by the larger I_E/I_M ratio in Figure 4 and the larger $\langle k_{blob} \times N_{blob} \rangle$ or $k_{cy} \times N$ products in Figure 8. Consequently, although specific solvent effects might be happening, their overall effect on the conclusions drawn from this study is expected to be small.

CONCLUSIONS

The LRPCD of PNIPAM were described in alcohol solvents for two series of pyrene-labeled PNIPAMs. The first series was constituted of five short monodisperse PNIPAMs end-labeled with pyrene. The second series was composed of five large polydisperse PNIPAMs randomly labeled with pyrene. The steady-state fluorescence spectra and time-resolved fluorescence decays of all samples were acquired and analyzed according to the Birks scheme for the end-labeled PNIPAMs and the FBM for the randomly labeled PNIPAMs. The main result of this study is the observation that the parameters describing the efficiency of pyrene excimer formation obtained by steady-state (I_E/I_M ratio in Figure 4A and the inset of Figure 4B) and time-resolved ($\langle k_{blob} \times N_{blob} \rangle$ and $\langle k_{cy} \times N \rangle$ in Figure 8) fluorescence compare remarkably well for the two types of constructs. This result demonstrates that the two types of PNIPAM constructs provide internally consistent information about the LRPCD of PNIPAM, a conclusion similar to the one reached for polystyrene in earlier publications.[11,45]

The products $k_{cy} \times N$ obtained for the end-labeled polymers and $k_{blob} \times N_{blob}$ obtained for the randomly labeled polymers were compared to gauge the relative flexibility of polystyrene with respect to PNIPAM. The relatively small differences found for the $k_{blob} \times N_{blob}$ and $k_{cy} \times N$ values between polystyrene and PNIPAM suggest that these polymers exhibit similar backbone flexibility, a conclusion which is both supported from the reported C_∞ values of the polymers[57,58] and reasonable considering the chemical structure of the structural units of the two polymers which bear side-chains of similar bulkiness.

The advantages of using randomly labeled polymers consist of their easier preparation by copolymerization or polymer postmodification, an enhanced excimer formation by reducing the average distance between every pair of pyrenes (cf. Figure 3, parts A and B, and ref 11), and not being limited to the use short chains (see complications to the Birks scheme in Figure 5 and ref 42). These advantages must be balanced with the disadvantage of using eqs S.5 and S.6 in the Supporting Information for the FBM which are mathematically more involved than eqs S.1 and S.2 in the Supporting Information typically used with end-labeled polymers. The advantages and disadvantages of each approach need to be carefully weighed by the experimentalist interested in characterizing the LRPCD of a given polymeric backbone. In any case, whatever the chosen approach is, the good agreement found for polystyrene[11,44−47] and now PNIPAM between $k_{cy} \times N$ for end-labeled monodisperse polymers and $k_{blob} \times N_{blob}$ for randomly labeled polydisperse polymers demonstrate that randomly labeled polymers constitute an appealing alternative to end-labeled polymers to study LRPCD by fluorescence.

ASSOCIATED CONTENT

Supporting Information. Description of the Birks scheme and FBM, tables summarizing the parameters used to described the kinetics of excimer formation, parameters retrieved from the analysis of the fluorescence decays, plots of $\langle k_{cy} \times N \rangle$ versus the inverse of viscosity for PEO, PNIPAM, and PS, and errors on the exponents given in Figure 5. This material is available free of charge via the Internet at http://pubs.acs.org.

ACKNOWLEDGMENT

Both research groups thank the NSERC for generous funding.

REFERENCES

(1) Cuniberti, C.; Perico, A. *Eur. Polym. J.* **1977**, *13*, 369–374.
(2) Cuniberti, C.; Perico, A. *Eur. Polym. J.* **1980**, *16*, 887–893.
(3) Winnik, M. A.; Redpath, T.; Richards, D. H. *Macromolecules* **1980**, *13*, 328–335.
(4) Cuniberti, C.; Perico, A. *Prog. Polym. Sci.* **1984**, *10*, 271–316.
(5) Winnik, M. A. *Acc. Chem. Res.* **1985**, *18*, 73–79.
(6) Duhamel, J. in *Molecular interfacial phenomena of polymers and biopolymers*; Chen, P., Ed., Woodhead; New York, 2005.
(7) Duhamel, J. *Acc. Chem. Res.* **2006**, *39*, 953–960.
(8) Wilemski, G.; Fixman, M. *J. Chem. Phys.* **1974**, *60*, 866–877.
(9) Wilemski, G.; Fixman, M. *J. Chem. Phys.* **1974**, *60*, 878–890.
(10) Birks, J. B. *Photophysics of Aromatic Molecules*; Wiley: New York, 1970; p 301.
(11) Ingratta, M.; Hollinger, J.; Duhamel, J. *J. Am. Chem. Soc.* **2008**, *130*, 9420–9428.
(12) Svirskaya, P.; Danhelka, J.; Redpath, A. E. C.; Winnik, M. A. *Polymer* **1983**, *24*, 319–322.
(13) Boileau, S.; Méchin, F.; Martinho, J. M. G.; Winnik, M. A. *Macromolecules* **1989**, *22*, 215–220.
(14) Ghiggino, K. P.; Snare, M. J.; Thistlethwaite, P. J. *Eur. Polym. J.* **1985**, *21*, 265–272.
(15) Cheung, S.-T.; Winnik, M. A.; Redpath, A. E. C. *Makromol. Chem.* **1982**, *183*, 1815–1824.
(16) Slomkowski, S.; Winnik, M. A. *Macromolecules* **1986**, *19*, 500–501.
(17) Kim, S. D.; Torkelson, J. M. *Macromolecules* **2002**, *35*, 5943–5952.
(18) Gardinier, W. E.; Bright, F. V. *J. Phys. Chem. B* **2005**, *109*, 14824–14829.
(19) Duhamel, J.; Khayakin, Y.; Hu, Y. Z.; Winnik, M. A.; Boileau, S.; Méchin, F. *Eur. Polym. J.* **1994**, *30*, 129–134.
(20) Lee, S.; Winnik, M. A. *Macromolecules* **1997**, *30*, 2633–2641.

(21) Lee, S.; Duhamel, J. *Macromolecules* **1998**, *31*, 9193–9200.
(22) Farinha, J. P. S.; Piçarra, S.; Miesel, K.; Martinho, J. M. G. *J. Phys. Chem. B* **2001**, *105*, 10536–10545.
(23) Piçarra, S.; Gomes, P. T.; Martinho, J. M. G. *Macromolecules* **2000**, *33*, 3947–3950.
(24) Costa, T.; Seixas de Melo, J.; Burrows, H. D. *J. Phys. Chem. B* **2009**, *113*, 618–626.
(25) Winnik, M. A.; Basu, S. N.; Lee, C. K.; Saunders, D. S. *J. Am. Chem. Soc.* **1976**, *98*, 2928–2935.
(26) Horie, K.; Schnabel, W.; Mita, I.; Ushiki, H. *Macromolecules* **1981**, *14*, 1422–1428.
(27) Lee, S.; Winnik, M. A. *Can. J. Chem.* **1993**, *71*, 1216–1224.
(28) Lee, S.; Winnik, M. A. *Can. J. Chem.* **1994**, *72*, 1587–1595.
(29) Eaton, W. A.; Muñoz, V.; Hagen, S. J.; Jas, G. S.; Lapidus, L. J.; Henry, E. R.; Hofrichter, J. *Annu. Rev. Biophys. Biomol. Struct.* **2000**, *29*, 327–359.
(30) Hagen, S. J.; Hofrichter, J.; Szabo, A.; Eaton, W. A. *Proc. Natl. Acad. Sci. USA* **1996**, *93*, 11615–11617.
(31) McGimpsey, W. G.; Chen, L.; Carraway, R.; Samaniego, W. N. *J. Phys. Chem. A* **1999**, *103*, 6082–6090.
(32) Möglich, A.; Krieger, F.; Kiefhaber, T. *J. Mol. Biol.* **2005**, *345*, 153–162.
(33) Fierz, B.; Satzger, H.; Root, C.; Gich, P.; Zinth, W.; Kiefhaber, T. *Proc. Natl. Acad. Sci. USA* **2007**, *104*, 2163–2168.
(34) Möglich, A.; Joder, K.; Kiefhaber, T. *Proc. Natl. Acad. Sci. U.S.A.* **2006**, *103*, 12394–12399.
(35) Hudgins, R. R.; Huang, F.; Gramlich, G.; Nau, W. M. *J. Am. Chem. Soc.* **2002**, *124*, 556–564.
(36) Huang, F.; Hudgins, R. R.; Nau, W. M. *J. Am. Chem. Soc.* **2004**, *126*, 16665–16675.
(37) Roccatano, D.; Sahoo, H.; Zacharias, M.; Nau, W. M. *J. Phys. Chem. B* **2007**, *111*, 2639–2646.
(38) Bieri, O.; Wirz, J.; Hellrung, B.; Schutkowski, M.; Drewello, M.; Kiefhaber, T. *Proc. Natl. Acad. Sci.* **1999**, *96*, 9597–9601.
(39) Krieger, F.; Fierz, B.; Bieri, O.; Drewello, M.; Kiefhaber, T. *J. Mol. Biol.* **2003**, *332*, 265–274.
(40) Lapidus, L. J.; Eaton, W. A.; Hofrichter, J. *Proc. Natl. Acad. Sci. U.S.A.* **2000**, *97*, 7220–7225.
(41) Neuweiler, H.; Löllmann, M.; Doose, S.; Sauer, M. *J. Mol. Biol.* **2007**, *365*, 856–869.
(42) Chen, S.; Duhamel, J.; Winnik, M. A. *J. Phys. Chem. B* **2011**, *115*, 3289–3302.
(43) Mathew, A.; Siu, H.; Duhamel, J. *Macromolecules* **1999**, *32*, 7100–7108.
(44) Ingratta, M.; Duhamel, J. *Macromolecules* **2007**, *40* (18), 6647–6657.
(45) Ingratta, M.; Duhamel, J. *Macromolecules* **2009**, *42* (4), 1244–1251.
(46) Ingratta, M.; Duhamel, J. *J. Phys. Chem. B* **2009**, *113*, 2284–2292.
(47) Ingratta, M.; Mathew, M.; Duhamel, J. *Can. J. Chem.* **2010**, *88*, 217–227.
(48) Kanagalingam, S.; Ngan, C. F.; Duhamel, J. *Macromolecules* **2002**, *35*, 8560–8570.
(49) Kanagalingam, S.; Spartalis, J.; Cao, T.-C.; Duhamel, J. *Macromolecules* **2002**, *35*, 8571–8577.
(50) Irondi, K.; Zhang, M.; Duhamel, J. *J. Phys. Chem. B* **2006**, *110*, 2628–2637.
(51) Teertstra, S. J.; Lin, W. Y.; Gauthier, M.; Ingratta, M.; Duhamel, J. *Polymer* **2009**, *50*, 5456–5466.
(52) Yip, J.; Duhamel, J.; Qiu, X.; Winnik, F. M. *Can. J. Chem.* **2011**, *89*, 163–172.
(53) Winnik, F. M. *Macromolecules* **1990**, *23*, 233–242.
(54) Qiu, X. P.; Winnik, F. M. *Macromolecules* **2007**, *40*, 872–878.
(55) Sequi, F.; Qiu, X. P.; Winnik, F. M. *J. Polym. Sci., Part A* **2008**, *46*, 314–326.
(56) Molar absorption coefficient was determined in the laboratory.
(57) Bandrup, J. ; Immergut, E. H.; Grulke, E. A. *Polymer Handbook*, 4th ed.; John Wiley & Sons: New York, 1999; p VII 675−683.
(58) Fang, Z.; Zhen, T.; Sato, T. *Sci. China B* **1999**, *42*, 290–297.
(59) Flory, P. J. *Statistical Mechanics of Chain Molecules*; Interscience: New York, 1969.